

Concentration of algal cells for Raman analysis by electrowetting on dielectrics (EWOD)

Abstract

In this study, electrowetting on dielectric (EWOD) was applied to a droplet of particle or algal solution to 1) suppress the coffee ring effect occurred during evaporation process, 2) concentrate the particle or algal cells and 3) shorten the processing time for analysis. The results showed that the micro particles and algal cells were effectively concentrated within approximately 15 minutes on the Teflon-coated microchip with interdigitated electrodes operated at the applied frequencies around 1k Hz and voltage 300 Vpp. The evaporation time for the sessile drop decreased substantially when applying EWOD and the size of the spot could be reduced to approximately 16% of that of the initial droplet. For algal solution with OD682 value equal to 5.32, strong Raman signals of microalgae were obtained near the central region of the dried algal spot.

Keywords: electrowetting on dielectric (Ewod), microalgae, lipid, carotenoid, Raman spectroscopy

Volume 2 Issue 1 - 2017

Bo Syu Shen, Yi Je Juang

Department of Chemical Engineering, National Cheng Kung University, Taiwan

Correspondence: Yi-Je Juang, Department of Chemical Engineering, National Cheng Kung University, No. 1 University Road, Tainan, Taiwan, Tel +886-6-2757575 ext 62653, Fax +886-6-2344496, Email yijuang@mail.ncku.edu.tw

Received: October 20, 2016 | **Published:** January 04, 2017

Abbreviations: Ewod, electrowetting on dielectric; Ito, indium tin oxide; Peg, polyethylene glycol; Ps, polystyrene; Od, optical density

Introduction

Among various types of renewable energy, bio fuel is receiving more and more attention and has become one of the promising energy sources for the future energy application. Utilization of the microalgae as a source for bio fuel production offer many merits such as high lipid content, high growth rate, no need to compete with arable land,¹ higher energy density,² absorbing carbon dioxide to mitigate global warming and producing other valued compounds. In order for successful commercialization of bio fuel, one of the important steps is to be able to quantify the lipid content inside the microalgae in a rapid fashion such that screening of lipid-rich algal strains in a timely manner, optimization of the cultivation conditions and on-site monitoring of the cultivation process become feasible. For conventional techniques used to quantify the microalgae cellular lipids such as gas chromatography (GC) analysis and gram measurement,³⁻⁵ they are typically invasive, time-consuming, and involved in expensive instrument and well-trained personnel. The lipid-conjugated fluorescent dye such as Nile red and BODIPY 505/515 was used to quantify the lipid content through fluorescence intensity analysis and similar results can be achieved compared to those from conventional techniques.⁶⁻⁸ Raman spectroscopy, a powerful tool to determine chemical composition of materials, has been utilized to characterize many biological systems.⁹ This is because the Raman signal of water is weak and uncomplicated, the sample can be analyzed in-vivo, and sample preparation is generally not required.¹⁰ Identification of algae species,^{11,12} probing the influence of environment on microalgae,¹³ quantification of degree of unsaturation¹⁴ and β -carotene¹⁵ in the lipid bodies, etc. have been reported. Recently, rapid quantification of lipid content inside microalgae using Raman spectroscopy has been demonstrated.¹⁶ The algal paste was first prepared after 1-hour evaporation of an algal droplet on a gold coated glass slide, followed

by applying near-infrared Raman spectrometry. The method provided representative information of a microalgae culture through cell ensemble measurements and shortened the time for quantification to less than 1.5 h. However, the coffee ring effect during droplet evaporation leads to an undesired inhomogeneous deposition of algal cells distributed across the algal paste. As a consequence, the signal intensity will vary from one location to another and searching for “hot spots” on the algal paste to provide strong signals is inevitable. The coffee ring effect is a phenomenon which results from pinning of the three-phase contact line and a convective flux driven by evaporation brings the solute to deposit in a ring at the edge.¹⁷ Several approaches have been proposed to suppress the coffee ring effect like making the substrate surface super hydrophobic,¹⁸ generating Marangoni flow,¹⁹ utilizing the electric field,²⁰⁻²² adjusting the viscosity and drying time of the droplet,²³ and applying electrowetting on dielectric (EWOD) at the sessile drop.²⁴ For applying EWOD to suppress the coffee ring effect, there are several advantages such as working for DI water, no need of adding additives in the solution, generating no heat in the droplet and the sessile drop not being in direct contact with the electrodes.²⁴ The mechanism of suppressing the coffee ring effect by applying EWOD is to excite the sessile drop to oscillate using alternating voltage (AC) over a wide frequency range.²⁵ This leads to generation of internal flow inside the sessile drop which inhibit the solute to deposit at the three-phase contact line. The internal flow can be either hydrodynamic at lower driving frequency or electro thermal at higher driving frequency.²⁶ With this strategy, suppression of coffee ring effect was effective and concentration of polystyrene particles, c DNA and PEG molecules was demonstrated.^{24,27} In this study, the particle solution was used to address the effect of the different processing parameters such as applied voltage, frequency, droplet volume and volume fraction of the particle droplet on suppressing the coffee ring effect. Then electrowetting on dielectric (EWOD) was applied to a droplet of algal solution to concentrate the algal cells for better acquiring the Raman signals and shorten the sample preparation time. Comparison of the Raman signals obtained with and without applying EWOD is made.

Materials and methods

Materials

Teflon®AF 1601S was purchased from Dupont. The indium tin oxide (ITO) glass was purchased from Aim Core Technology (Taiwan) and the ITO etchant was purchased from Taimax (Taiwan). The fluorescent polystyrene micro particles with 5 μm in diameter were purchased from Thermo Fisher Scientific. The algal cells (*Chlorella vulgaris*) were cultivated according to the literature.²⁸ The algal solution was further diluted with deionized water to obtain the test samples with different optical densities (ODs).

Fabrication of microchips to perform EWOD:

To fabricate the EWOD chips, indium tin oxide (ITO) coated glass slides with patterned electrodes defined by photolithographic technique went through the etching process to obtain the interdigitated electrodes with 60 μm in width, 60 μm in spacing and 1.5 cm in length. Then the patterned glass slides were spin coated with Teflon®AF as the dielectric layer. Algal droplets with different OD values or droplets of particle solution with volume fraction ranging from 0.1 to 1 % were dispensed on the EWOD chip, which was connected to an AC function generator (AFG3101C, Tektronic) with the applied voltage between 250–450 Vpp and at frequencies from 300 to 10 kHz. The sizes of the droplets were measured and the flow behavior of the micro particles and algal cells were monitored as a function of time by using the inverted fluorescence microscopy (TE-2000S, Nikon).

Raman analysis:

The dried algal paste (either by evaporation or applying EWOD) on the ITO glass was analyzed by confocal microscopic Raman system (Thermo DXR Raman) with 532 nm laser. The laser power ranged from 0.5 to 5 mW and the exposure time was set at 1 sec. To acquire the Raman spectra, the signals were collected 10 times and the intensity was calculated with the unit of counts per second. The uniformity of the algal paste was examined by the Raman mapping and line scanning where the sampled area is around 0.5 mm \times 0.5 mm.

Results and discussion

From the literature, it was reported that the coffee ring effect resulted from undisturbed natural evaporation of a droplet with particle volume fraction ranging from 0.0007 to 0.6 % can be suppressed by applying EWOD at frequency around 1000 Hz and voltage 300 Vpp.²⁷ Figure 1 shows aggregation of the fluorescent PS particles with and without applying EWOD. τ is the time normalized by the total evaporation time, t_f . For droplet evaporation with and without applying EWOD in this study, t_f are approximately 15 and 60 min, respectively. It can be seen that, for undisturbed natural evaporation (0 V), the coffee ring was observed and the spot size remained similar to that of the initial droplet. On the other hand, when applying EWOD (300 Vpp), the size of the evaporating droplet gradually decreased as the time progressed and the particles were concentrated at a smaller area, indicating that the coffee ring effect was effectively suppressed. The effect of the applied frequency on the size of the evaporating droplet was examined as shown in Figure 2. At lower frequency (e.g. 300 Hz), the size of the evaporating droplet decreased but remained unchanged after τ around 0.4. As the frequency increases, the size of the evaporating droplet decreased monotonically and the normalized diameter of the spot reached to a minimum around 0.4. When the frequency further increased, the normalized diameter of the spot

increased again and it became 1 (i.e. spot size equal to the initial size of the droplet) at the applied frequency 10 kHz. It was reasoned that, at lower frequency, the internal flow was close to quasi-static and the drop shape between the spreading and receding phase was relatively symmetric. This led to a small, internal, net flow,²⁵ which could still prevent the contact line from pinning. After certain time, evaporation of the droplet caused the increase of particle volume fraction, which resulted in reduced net flow and pinning of the contact line. At higher frequency, the amplitude of the contact line motion disappears due to the inertia of the fluid.²⁵ Therefore, there was no net flow and the spot size was nearly the same as that of the initial droplet. This is in agreement with the literature that high drift velocity (or net flow) occurs at the intermediate frequencies.²⁵ It is worthy of mentioning that the particles were aligned along the electrodes, which is a result of dielectrophoresis.²⁹

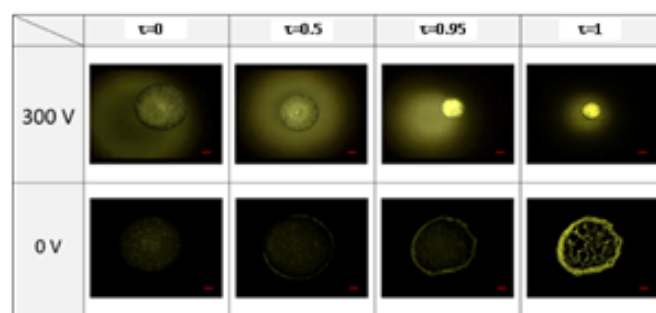


Figure 1 The particle aggregation by applying EWOD and natural evaporation (droplet volume: 1 μl ; volume fraction of particle solution: 0.1%; particle size: 4.8 μm ; frequency: 1000 Hz).

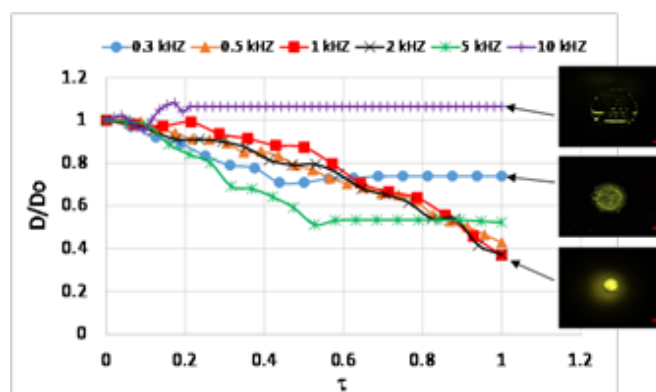


Figure 2 Normalized diameter (D/D_0) of evaporating drop at different applied frequencies (D_0 : diameter of the initial droplet; droplet volume: 1 μl ; voltage: 300 Vpp; particle size: 4.8 μm ; volume fraction of particle solution: 0.1%).

Figure 3 shows the effect of the applied voltage on the size of the evaporating droplet. It can be seen that, for lower voltage (e.g. 270 Vpp), the coffee ring effect became less profound compared to undisturbed natural evaporation and the spot size was reduced. Increase of the applied voltage to 300 Vpp showed a successful suppression of the coffee ring effect and the spot size was reduced to a minimum, where the particles were aggregated and concentrated within approximately 16% of the initial droplet area. As the applied voltage further increased, the normalized diameter of the spot increased again. It is hypothesized that, although there might be higher net flow due to the higher applied voltage, Joule heating might lead to faster evaporation of the droplet such that the spot size could not be reduced successfully.

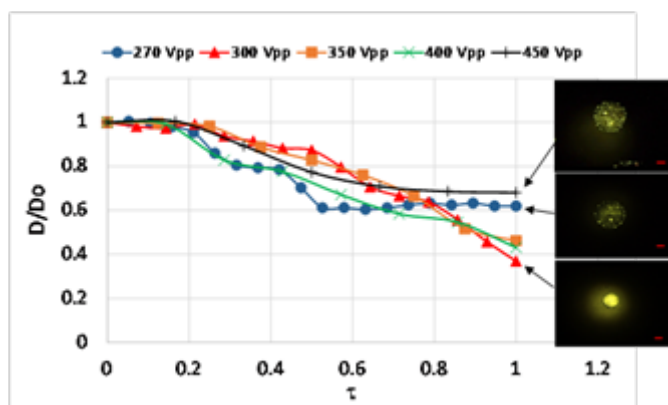


Figure 3 Normalized diameter (D/D_0) of an evaporating drop at different applied voltage (D_0 : diameter of the initial droplet; droplet volume: $1\mu\text{l}$; frequency: 1kHz ; particle size: $4.8\mu\text{m}$; volume fraction of particle solution: 0.1%).

Regarding the effect of droplet volume, it was found that the larger the droplet volume, the longer the evaporation time when the volume was less than $5\mu\text{l}$. If the evaporation time was normalized, it is interesting to see that the trends of the normalized diameter of the evaporating droplet are similar to each other as shown in Figure 4. This implied that the same evaporation mechanism by EWOD was applied despite different volumes of the droplets. Note that when the volume was larger than $5\mu\text{l}$, the evaporation time became substantially long and the working electrodes were damaged during evaporation process. Figure 5 shows the effect of volume fraction on the size of the evaporating droplet. It can be seen that evaporation of the droplets with volume fractions ranging from 0.1 to 1% yielded the similar normalized diameter, i.e. 0.4 and the fluorescent intensity of the spot increased as the volume fraction increased.

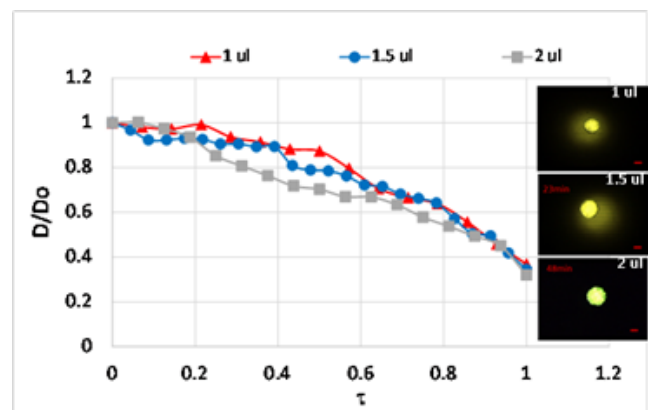


Figure 4 Normalized diameter (D/D_0) of evaporating drop for different droplet volume (D_0 : diameter of the initial droplet; voltage: 300Vpp ; frequency: 1kHz ; particle size: $4.8\mu\text{m}$; volume fraction of particle solution: 0.1%).

Figure 6 shows the evaporation of algal droplet with and without applying EWOD. Compared to undisturbed natural evaporation, the size of the evaporating algal droplet by applying EWOD was reduced and the algal cells were successfully concentrated at a smaller region. It was found that the normalized diameter of the algal spot was approximately 0.4 , which is close to that of the spot of aggregated micro particles abovementioned. In fact, the trends of the evaporating droplets were nearly overlapped with each other for algal cells and micro particles as shown in Figure 7. It was noted that the algal cells do not seem to have any changes or be lysed at such high applied voltage. This could be that the electrical resistance of the cell wall

is much smaller than that of the cell membrane. Therefore, there is a smaller electric field within the cell wall and the irreversible dielectric breakdown of the cell wall did not occur.³⁰ Or it could be that the applied frequency is too low (compared to 600kHz in the literature) such that the electrical potential in the suspending medium is reduced owing to electrode polarization.³¹ Figure 8 shows the confocal mapping of the algal spot for algal droplet with different OD values. For OD value equal to 1.34 , although the coffee ring effect was still effectively suppressed by EWOD, the empty areas (i.e. the light color in the optical image) were clearly observed and scattered throughout the algal spot. This indicates that the number of algal cells is not sufficient to provide a good coverage on the substrate. For OD value equal to 2.68 , inhomogeneous deposition of algal cells was still observed although the coverage of the algal cells on the substrate was significantly improved. As the OD value increased to 5.32 , the highest signal intensity was found near the central region, indicating that the algal cells were indeed concentrated and better coverage was obtained near the central region of the substrate. Since the EWOD microchip was coated with Teflon as the dielectric layer, the Raman signals of the substrate were acquired as shown in Figure 9A. It can be seen that the background signals were not strong and the characteristic peaks at 585 and 1110cm^{-1} for ITO glass³² and at 734cm^{-1} for Teflon³³ were observed. These peaks will not interfere or overlap with those characteristic peaks of lipids ($1440, 1650\text{cm}^{-1}$) and carotenoids ($1160, 1537\text{cm}^{-1}$).³⁴ Figure 9B shows the Raman spectra of the microalgae. For evaporation by applying EWOD, it can be seen that clear Raman signals were obtained at the central region of the algal spot. As to undisturbed natural evaporation, comparable Raman signals were obtained only at the outside ring of the algal spot and either weaker or no signals were detected at the rest of the area.

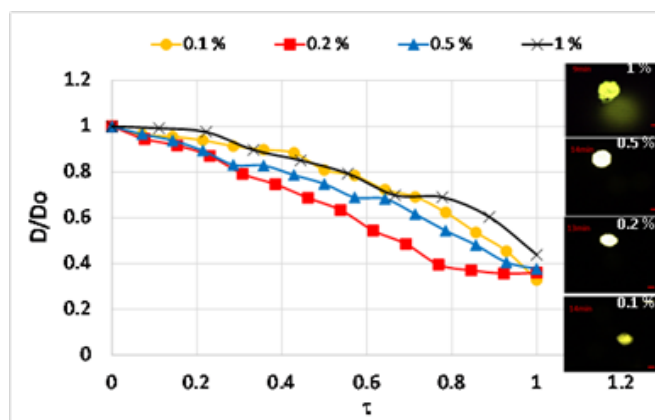


Figure 5 Normalized diameter (D/D_0) of evaporating drop for different volume fraction (D_0 : diameter of the initial droplet; droplet volume: $1\mu\text{l}$; voltage: 300Vpp ; frequency: 1kHz ; particle size: $4.8\mu\text{m}$).

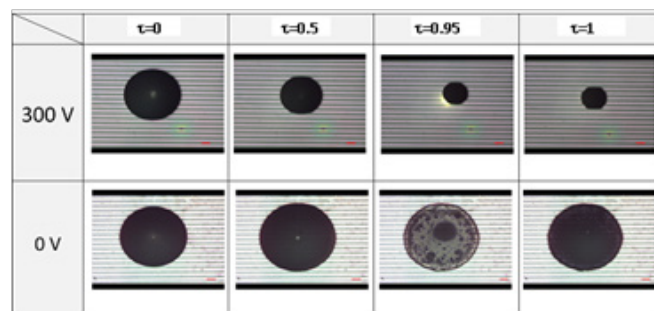


Figure 6 The microalgae aggregation by applying EWOD and natural evaporation (droplet volume: $1\mu\text{l}$; algae concentration: $\text{OD}_{682} : 5.32$).

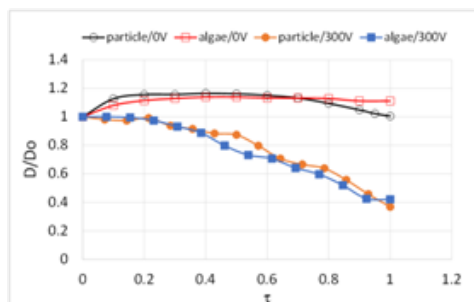


Figure 7 Compare fluorescent particles with algal cells concentrated with and without EWOD (droplet volume: 1 μ l; voltage: 300Vpp; frequency 1kHz; volume fraction of particle solution: 0.1%; algae concentration: OD₆₈₂ : 5.32).

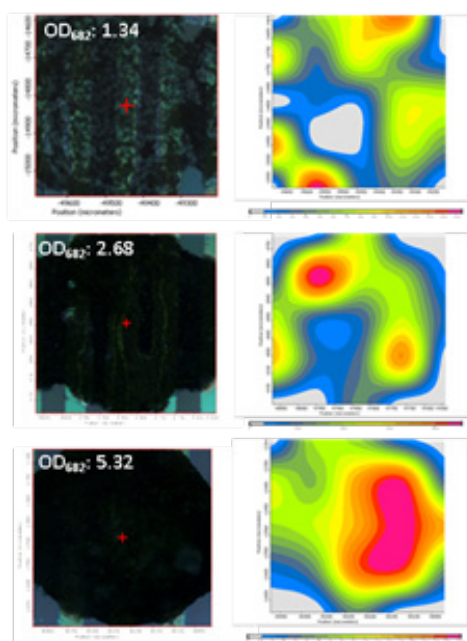


Figure 8 Confocal mapping of concentrated algal cells with different OD values. (Left column: optical image. Right column: Raman confocal mapping. Laser power intensity: 0.5mW; exposure time: 1 second).

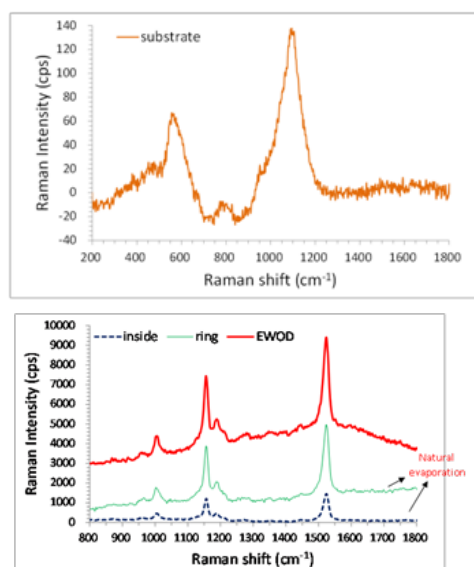


Figure 9 Raman spectrum of (A) EWOD microchip and (B) algal spots prepared by applying EWOD and natural evaporation. (Wavelength: 532 nm; Laser power intensity: 5mW; exposure time: 1 second; 10 accumulations).

Conclusion

In this study, electrowetting on dielectric (EWOD) was applied to the micro particle or algal droplet. The results showed that the coffee ring effect was effectively suppressed when applying EWOD on the droplet. For 1 μ l droplet with volume fraction 0.1 %, both the micro particles and algal cells were concentrated within 15 minutes at applied voltage 300Vpp and frequency 1kHz and the size of the spot was 16% of that of the initial droplet. For algal solution with OD value equal to 5.32, the algal cells were concentrated near the central region by EWOD and clear Raman signals were obtained.

Acknowledgements

The authors thank for the financial support from Ministry of Science and Technology in Taiwan (MOST 104-2221-E-006-230, 105-2221-E-006-228) and National Cheng Kung University (NCKU's "Top University" grant).

Conflict of interest

The author declares no conflict of interest.

References

- Ahmad AL, Mat Yasin NH, Derek CJC, et al. Microalgae as a sustainable energy source for biodiesel production: A review. *Renew Sust Energ Rev*. 2011;15(1):584–593.
- Waltz E. Plant genomics land big prizes. *Nat Biotechnol*. 2009;27:5.
- Montero MF, Aristizabal M, Reina GG. Isolation of high-lipid content strains of the marine microalga *Tetraselmis suecica* for biodiesel production by flow cytometry and single-cell sorting. *J Appl Phycol*. 2011;23 (6):1053–1057.
- Priscu JC, Priscu LR, Palmisano AC, et al. Estimation of neutral lipid levels in Antarctic sea-ice microalgae by Nile red fluorescence. *Antarct Sci*. 1990;2(2):149–155.
- Bligh EG. Rapid method of total lipid extraction and purification. *Can J Biochem Physiol*. 1978;37:911–917
- Mutanda T, Ramesh D, Karthikeyan S, et al. Bio prospecting for hyper-lipid producing micro algal strains for sustainable bio fuel production. *Bioresour. Technol*. 2011;102(1):57–70.
- Cooper MS, Hardin WR, Petersen TW, et al. Visualizing "green oil" in live algal cells. *J Biosci Bioeng*. 2010;109(2):198–201.
- Chen W, Zhang C, Song L, et al. A high throughput Nile red method for quantitative measurement of neutral lipids in microalgae. *J Microbiol Methods*. 2009;77(1):41–47.
- Pappas D, Smith BW, Winefordner JD. Raman spectroscopy in bioanalysis. *Talanta*. 2000;51(1):131–144.
- Parab NDT, Tomar NDT. Raman spectroscopy of algae: A review. *J Nanomedic Nanotechnol*. 2012;3(2):131.
- Brahma SK, Hargraves PE, Howard WF, et al. A resonance Raman method for the rapid detection and identification of algae in water. *Appl Spectrosc*. 1983;37(1):55–58.
- Ramya S, George RP, Rao SRV. et al. Differentiation of alga clones on the basis of resonance Raman spectra excited by visible light. *Anal Chem*. 1998;70(9):1782–1787.
- Heraud P, Wood BR, Beardall J. et al. *New approaches in biomedical spectroscopy*. New York, USA: American chemical society; 2007. p. 85–106.
- Samek O, Jonas A, Pilat Z, et al. Raman micro spectroscopy of individual algal cells: Sensing unsaturation of storage lipids *in vivo*. *Sensors*. 2010;10(9):8635–8651.

15. Pilat Z, Bernatova S, J Jezek, et al. Raman micro spectroscopy of algal lipid bodies: β -carotene quantification. *J Appl Phycol*. 2012;24(3):541–546.
16. Lee TH, Chang JS, Wang HY. Rapid and *in vivo* quantification of cellular lipids in *Chlorella vulgaris* using near-infrared Raman spectrometry. *Anal Chem*. 2013;85(4):2155–2160.
17. Deegan RD, Bakajin O, Dupont TF, et al. Capillary flow as the cause of ring stains from dried liquid drops. *Nature*. 1997;389:827–829.
18. Kuncicky DM, Velez OD. Surface-guided templating of particle assemblies inside drying sessile droplets. *Langmuir*. 2008;24(4):1371–1380.
19. Hu H, Larson RG. Marangoni effect reverses coffee-ring depositions. *J Phys Chem B*. 2006;110(14):7090–7094.
20. Kim SJ, Kang KH, Lee JG, et al. Control of particle-deposition pattern in a sessile droplet by using radial electroosmotic flow. *Anal Chem*. 2006;78(14):5192–5197.
21. Orejon D, Sefiane K, Shanahan ME. Evaporation of nano fluid droplets with applied DC potentials. *J Colloid Interface Sci*. 2013;407:29–38.
22. Wray AW, Papageorgiou DT, Craster RV, et al. Electrostatic suppression of the “coffee stain effect”. *Langmuir*. 2014;30(20):5849–5858.
23. Friederich A, Binder JR, Bauer W. Rheological control of the coffee stain effect for inkjet printing of ceramics. *J Am Ceram Soc*. 2013;96(7):2093–2099.
24. Eral HB, Mampallil Augustine D, Duits MHG, et al. Suppressing the coffee stain effect: How to control colloidal self-assembly in evaporating drops using electrowetting. *Soft Matter*. 2011;7(10):4954–4958.
25. Mugele F, Staicu A, Bakker R, et al. Capillary stokes drift: A new driving mechanism for mixing in AC-electrowetting. *Lab Chip*. 2011;11(12):2011–2016.
26. Mampallil D, Tiwari D, van den Ende D, et al. Sample pre concentration inside sessile droplets using electrowetting. *Biomicrofluidics*. 2013;7(4):044102.
27. Mampallil D, Eral HB, van den Ende D, et al. Control of evaporating complex fluids through electrowetting. *Soft Matter*. 2012;8:10614–10617.
28. Yeh KL, Chang JS. Nitrogen starvation strategies and photo bioreactor design for enhancing lipid content and lipid productivity of a newly isolated microalga *Chlorella vulgaris* ESP-31. *Biotechnol J*. 2011;6(11):1358–1366.
29. Mugele F, Baret JC. Electrowetting: from basics to applications. *J Phys Condens Matter*. 2005;17:R705–774.
30. Azencott HR, Peter GF, Prausnitz MR. Influence of the cell wall on intracellular delivery to algal cells by electro poration and sonication. *Ultrasound Med Biol*. 2007;33(11):1805–1817.
31. Bahi MM, Tsaloglou MN, Mowlem M, et al. Electro poration and lysis of marine microalga *Karenia brevis* for RNA extraction and amplification. *J R Soc Interface*. 2011;8(57):601–608.
32. Chandrasekhar R, Choy KL. Innovative and cost-effective synthesis of indium tin oxide films. *Thin Solid Films*. 2011;398-399:59–64.
33. Lobo H, Bonilla JV. *Handbook of Plastic Analysis*. New York: Marcel Dekker Inc; 2003.
34. Wu H, Volponi JV, Oliver AE, et al. *In vivo* lipidomics using single-cell Raman spectroscopy. *P Natl Acad Sci USA*. 2011;108(9):3809–3814.